

AD-A285 076



AFOSR-TM 94 0570  
Dist: A  
①

*Final Technical Report*

*AFOSR Contract No. 90-0241*

*Resonance Enhanced Multiphoton Ionization*

*of*

*Molecules and Molecular Fragments*

*Vincent McKoy*

*A.A. Noyes Laboratory of Chemical Physics*

*California Institute of Technology*

*Pasadena, CA 91125*

PTI  
SEP 3 9 1994  
3 0 3 0

*Period: June 1, 1990 - March 31, 1994*

*Attn.: Dr. Michael Berman*

*AFOSR*

*Bolling AFB, DC*

94-31011



94 9 28 047

Dist: A

## REPORT DOCUMENTATION PAGE

Form Approved  
OMB No. 0704-0188

PLANE REPORTING BURDEN FOR THE COLLECTION OF INFORMATION IS ESTIMATED TO AVERAGE 1 HOUR PER RESPONSE, INCLUDING THE TIME FOR REVIEWING INSTRUCTIONS, SEARCHING EXISTING DATA SOURCES, GATHERING AND MAINTAINING THE DATA NEEDS, AND COMPUTING AND REVIEWING THE COLLECTION OF INFORMATION. SEND COMMENTS REGARDING THIS BUREAU'S ESTIMATE OR ANY OTHER ASPECT OF THE COLLECTION OF INFORMATION, INCLUDING SUGGESTIONS FOR REDUCING THIS BURDEN, TO Washington Headquarters Services, Directorate for Information Operations and Strategy, 1215 Jefferson Davis Highway, Suite 1302, Arlington, VA 22202-4302, and to the Office of Management and Budget, Paperwork Reduction Project (0704-0188), Washington, DC 20503.

1. AGENCY USE ONLY (Leave Blank)	2. REPORT DATE	3. REPORT TYPE AND DATES COVERED
		Final - 1 Jun 90 - 31 Mar 91
4. TITLE AND SUBTITLE		5. FUNDING NUMBERS
Resonance Enhanced Multiphoton Ionization of Molecules and Molecular Fragments		AFOSR-90-C-241
6. AUTHOR(S)		61102F
Vincent McKoy		2303-FS
7. PERFORMING ORGANIZATION NAME(S) AND ADDRESS(ES)		8. PERFORMING ORGANIZATION REPORT NUMBER
California Institute of Technology Pasadena, CA 91125		8404547
9. SPONSORING/MONITORING AGENCY NAME(S) AND ADDRESS(ES)		10. SPONSORING/MONITORING AGENCY REPORT NUMBER
AFOSR/NP NL Bolling AFB, Washington, DC 20332-6448		
Dr. Betman		
11. SUPPLEMENTARY NOTES		
12a. DISTRIBUTION/AVAILABILITY STATEMENT		12b. DISTRIBUTION CODE
APPROVED FOR PUBLIC RELEASE DISTRIBUTION IS UNLIMITED		A
13. ABSTRACT (Maximum 200 words)		
<p>We have completed studies of ion rotational distributions produced by resonance enhanced multiphoton ionization of excited states of molecules and by single-photon ionization of ground states of jet-cooled molecules by coherent VUV radiation. The objective of this effort was to provide a robust analysis and prediction of key spectral features of interest in related experimental studies and technological applications of these laser-driven ionization techniques.</p> <p>Specific achievements include: (i) identification of underlying mechanisms for anomalous behavior of ion rotational distributions in laser ionization of molecules and molecular fragments, (ii) development of schemes for exploiting such anomalous behavior to achieve state-selective production of ions, and (iii) providing needed insight into the underlying dynamics of state-resolved molecular photoionization</p>		
DTIC QUALITY CONTROLLED 3		

14. SUBJECT TERMS	15. NUMBER OF PAGES
Multiphoton ionization of molecules; ultrasensitive detection of trace species; state-selected production of ions; dynamics of state-resolved molecular photoionization.	
16. PRICE CODE	
17. SECURITY CLASSIFICATION OF REPORT	18. SECURITY CLASSIFICATION OF THIS PAGE
UNCLASSIFIED	UNCLASSIFIED
19. SECURITY CLASSIFICATION OF ABSTRACT	20. LIMITATION OF ABSTRACT
UNCLASSIFIED	UL (UNLIMITED) SAR (SAME AS REPORT)

## I. Background and Objectives

Resonance enhanced multiphoton ionization (REMPI) utilizes laser radiation to prepare a molecule in an excited state via absorption of one or more photons and to subsequently ionize that level before it decays. A remarkable feature of REMPI is that the very narrow bandwidth of laser radiation makes it possible to select a specific rotational level in the initial (ground) state and to prepare the excited state of a species of interest in a single rotational level. Thus, by suitable choice of the excitation step, it is possible to selectively ionize a species which occurs in very minor concentrations, without ionizing any other species that may be present. *This conversion of optical selectivity into chemical selectivity makes REMPI one of the most powerful tools for ultrasensitive detection of species.* Other applications of REMPI include its use in studies of state-selected chemistry and for exploring excited-state chemistry and physics. Coupled with high-resolution photoelectron detection, REMPI also provides ion rotational distributions for ionization of single rotational levels of excited electronic states.

Although REMPI has the distinct advantage that a single rotational level of an excited state of a molecule is ionized and that it can be achieved with photon energies less than molecular ionization potentials and consequently at more convenient wavelengths than the vacuum ultraviolet (VUV) photons required for single-photon ionization, studies of single-photon ionization of ground states of jet-cooled molecules by coherent VUV and extreme ultraviolet (XUV) radiation are highly complementary to those of REMPI. The tunable coherent radiation required for these studies can be readily produced by third-harmonic generation as well as by four-wave sum or difference frequency mixing.<sup>1</sup>

Availability Codes	
Dist	Avail and/or Special
A-1	

The objective of our work has been to carry out quantitative theoretical studies of resonance enhanced multiphoton ionization of molecules and molecular fragments and single-photon ionization of such species by coherent VUV radiation so as to provide a robust description of key spectral features of interest in related experiments and applications and needed insight into the underlying dynamics of these spectra. A major focus of our work has been on joint theoretical and experimental studies of these laser-driven ionization processes. Many of these collaborations with experimental groups in the US, Canada, and the Netherlands stem primarily from the recent development of a technique, based on the detection of threshold or zero-kinetic-energy (ZEKE) photoelectrons resulting from pulsed field ionization (PFI) of very high Rydberg states lying below an ion rotational threshold, which *makes it possible to obtain ion rovibronic state distributions with sub-wavenumber resolution.*<sup>2</sup> The unprecedented resolution of this technique ( $1 \text{ cm}^{-1}$  or better) is opening up entirely new vistas in studies of ion spectroscopy, state-selective chemistry, and photoionization dynamics. Emerging applications built on the ultrahigh resolution of this technique include its use for accurate determination of thermochemically important ionization potentials, for characterization of ion rovibrational level structure of large organic molecules, elemental clusters, and weakly bound molecular complexes, and as a probe of nascent internal energy distributions of transient radicals.<sup>3</sup> This surge of experimental activity raises new theoretical challenges which have increasingly become the focus of our work.

## II *Highlights of Accomplishments*

In this section I will review the progress we have made in our studies of ion rotational distributions resulting from REMPI of molecules and from single-photon

ionization of jet-cooled molecules by coherent VUV and XUV radiation. This review is not intended to be exhaustive but to highlight the significance of our objectives and accomplishments and to illustrate the insight our studies provide.

Although we will not discuss the quantum mechanical formulation and computational procedures used to obtain the molecular photoelectron orbitals and photoionization matrix elements needed in these studies,<sup>4</sup> it is essential to recognize that the rotationally state-selective studies of interest here require the use of molecular photoelectron orbitals which correctly incorporate the angular momentum coupling present in these orbitals. In contrast to atomic photoelectron orbitals, molecular photoelectron orbitals are not angular momentum eigenfunctions but contain admixtures of angular momenta. This coupling of angular momenta is brought about by the torques associated with the nonspherical potentials of molecular ions in which the photoelectron moves. This simply reflects the fact that as the photoelectron scatters off the ion core, its angular momentum ( $\ell$ ) as well as that of the ion core (J) changes. These angular-momentum changing collisions between the photoelectron and the ion clearly play a crucial role in determining ion rotational distributions.

In these studies the molecular photoelectron orbitals are obtained as solutions of a one-electron Schrödinger equation containing the Hartree-Fock potential of the molecular ion  $V_{ion}$ , ( $\mathbf{r}, R$ ),

$$(-\frac{1}{2} \nabla^2 + V_{ion}(\mathbf{r}, R) - \frac{k^2}{2})\psi_{k\ell m}^{(-)}(\mathbf{r}, R) = 0, \quad (1)$$

where  $\psi_{k\ell m}^{(-)}$  is a partial wave component of the photoelectron orbital  $\Psi_k^{(-)}$ . The  $\psi_{k\ell m}^{(-)}$  satisfy scattering boundary conditions and must be obtained numerically. We actually obtain these orbitals using an iterative procedure, based on the Schwinger variational principle, to solve the integral equation associated with eq. (1).<sup>4</sup> The

procedure is numerically stable even at the very low photoelectron energies ( $\sim 0.05$  eV) often of interest in these studies.

(a) *Resonance Enhanced Multiphoton Ionization of Molecules and Fragments*

As our first example we look at the rotational distributions of ions for (2+1) REMPI of the NH and OH radicals.<sup>5,6</sup> Fig. 1 shows (a) measured and (b) calculated rotationally resolved photoelectron spectra along with (c) calculated photoelectron angular distributions for (2 + 1) REMPI via the R(12) branch of the  $f^1\Pi$  (3p $\sigma$ ) state of NH for the  $v^+ = 0$  and 1 levels of the ion. In these spectra the spin-orbit components of the  $X^2\Pi$  state of NH $^+$  and the parity components of the resonant and ionic states are not resolved. The calculated spectrum is also convoluted with a Gaussian detection function having a full-width at half-maximum (FWHM) of 30 meV. The most striking feature of these spectra is the appearance of strong  $\Delta N = N^+ - N = \text{even}$  peaks, particularly for  $\Delta N = 0$ , for photoionization of this 3p $\sigma$  Rydberg orbital of NH. On the basis of the simple selection rule  $\Delta N + \ell = \text{odd}$ ,<sup>6</sup> these even  $\Delta N (= 0, \pm 2)$  peaks must be associated with odd ( $\ell = 1, 3$ ) angular momentum components of the photoelectron matrix element. With its 67% p character one would expect significant contributions from the  $\ell = 0$  and 2 components of the photoelectron matrix element for ionization of this 3p $\sigma$  Rydberg orbital and hence strong odd  $\Delta N$  peaks.

It is clearly important to identify the underlying dynamical reason for the unusual behavior seen in these ion rotational distributions. Detailed calculations of these rotational distributions show that the strong even  $\Delta N$  peaks in these spectra are, in fact, due to the presence of a Cooper minimum in the  $\ell = 2$  component

of the photoionization matrix element.<sup>6</sup> Such a Cooper minimum occurs at a photoelectron kinetic energy where a specific angular momentum component of the photoionization matrix element changes sign and goes through a zero. These angular momentum components of the photoelectron matrix element are essentially

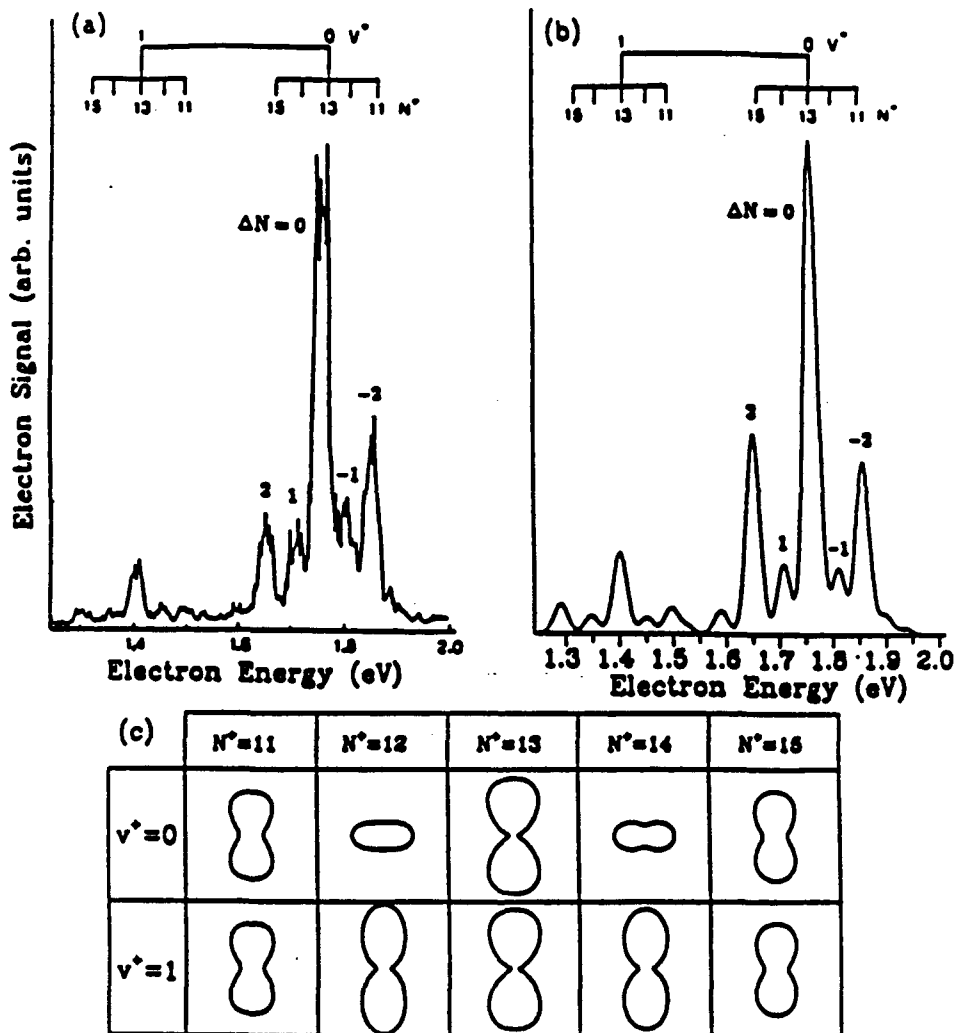


Fig. 1 (a) measured and (b) calculated photoelectron spectra along with the (c) calculated photoelectron angular distributions for  $(2 + 1)$  REMPI via the R(12) branch of the  $f^1\Pi$  ( $3p\sigma$ ) state of NH for the  $v^+ = 0$  and 1 vibrational bands. The measured spectra are taken from ref. 5.

the driving force for ejection of the photoelectron with a specific angular momentum  $\ell$ . At a Cooper minimum a specific  $\ell$  component of this driving force is diminished and hence corresponding ion rotational peaks, which are related to  $\ell$  through  $\Delta N + \ell = \text{odd}$ , are weakened. Here depletion of the d wave ( $\ell = 2$ ) contributions to the photoelectron matrix element in the vicinity of the Cooper minimum weakens the  $\Delta N = \text{odd}$  peaks and subsequently enhances the relative importance of the odd components ( $\ell = 1$  and 3) of this matrix element and, hence, that of the even  $\Delta N$  rotational peaks.

Fig. 1 (c) shows the calculated photoelectron angular distributions for the ion rotational levels in the spectrum of fig. 1. A significant feature of these spectra is that the angular distributions for the  $\Delta N = \pm 1$  peaks ( $N^+ = 12$  and 14) are quite different for the  $v^+ = 0$  and 1 levels of the ion. This behavior is due to a dependence of the photoelectron matrix element on internuclear distance which, in turn, arises from a rapid evolution the  $3p\sigma$  orbital of the  $f^1\Pi$  state from predominant 3p character at smaller internuclear distance to 3s character at larger R. It is surprising that this dependence is so evident for such low vibrational excitation.

Fig. 2 shows measured and calculated rotationally resolved photoelectron spectra for (2 + 1) REMPI of OH via the  $O_{11}$  (11) branch of the  $D^2\Sigma^-$  ( $3p\sigma$ ) [figs. 2 (a) and 2 (b)] and the  $3^2\Sigma^-$  ( $4s\sigma$ ) [figs. 2 (c) and 2 (d)] Rydberg states.<sup>7</sup> These spectra again serve to demonstrate the significant influence that Cooper minima exert on ion rotational distributions. Cooper minima have been predicted to occur in the d ( $\ell = 2$ ) wave of the  $k\sigma$  and  $k\pi$  continua for photoionization of the  $D^2\Sigma^-$  Rydberg state but not in the  $3^2\Sigma^-$  state. The presence of these Cooper minima for the  $D^2\Sigma^-$  state accounts for the occurrence of strong  $\Delta N = \text{even}$  signals in the photoelectron spectrum in contrast to the  $\Delta N = \text{odd}$  distribution expected for ionization

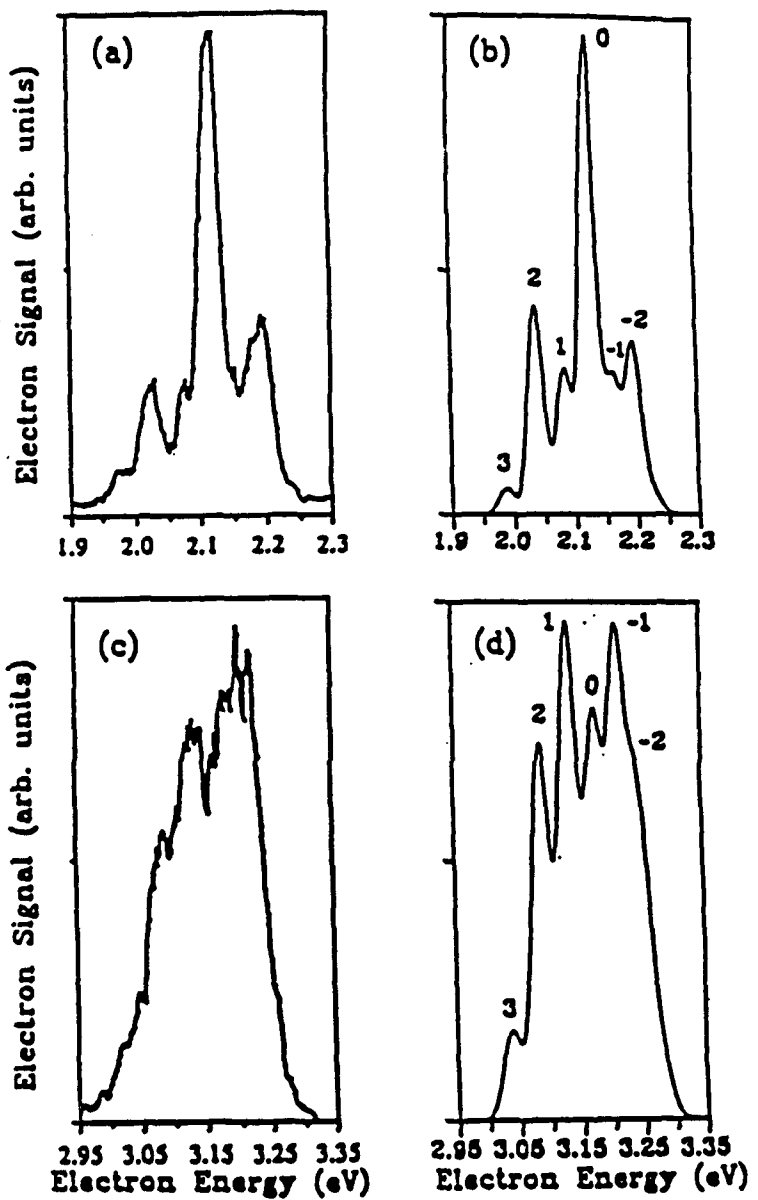


Fig. 2. Experimental and calculated rotationally resolved photoelectron spectra for (2 + 1) REMPI of OH: (a) measured spectrum for the  $D\ 2\Sigma^-$  photoelectron spectrum, assuming a Gaussian line shape with an FWHM of 30 meV; (c) measured spectrum for the  $3\ 2\Sigma^-$  ( $4s\sigma$ ) state,  $v = 0 \rightarrow v^+ = 0$ ,  $O_{11}$  (11) rotational branch; (d) calculated  $3\ 2\Sigma^-$  ( $4s\sigma$ ) photoelectron spectrum assuming a Gaussian line shape with a FWHM of 35 meV. The labelling of peaks in the calculated spectra indicates the change of rotational quantum number  $\Delta N = N^+ - N$ .

of a  $3p\sigma$  Rydberg orbital in an atomiclike picture, i.e.,  $3p\sigma \rightarrow ks, kd$  photoionizing transitions. On the other hand, the photoelectron spectra for photoionization of the  $3^2\Sigma^-$  ( $4s\sigma$ ) state of figs. 2(c) and 2(d) reveal a qualitatively different and much broader distribution with prominent  $\Delta N = \text{even}$  and  $\Delta N = \text{odd}$  transitions. The appearance of these spectra arises from greater  $\ell$ -mixing in this higher Rydberg orbital (54% s and 43% p character at  $R = 2.043 a_0$ ).

Cooper minima can be expected to have far-reaching and wide-spread implications for the behavior of ion rotational distributions. For example, similar effects in ion rotational distributions due to Cooper minima have also been predicted for H<sub>2</sub>O and SiF. Furthermore, Cooper minima can also be exploited to achieve a high degree of rotational selectivity in ion rotational distributions.<sup>8</sup>

We have also studied the rotational distributions of HBr<sup>+</sup> ions in their  $X^2\Pi_{1/2}$  ground state for (2 + 1) REMPI of HBr via the S(2) branch of the  $F^1\Delta_2$  (5p $\pi$ ) Rydberg state.<sup>9</sup> These studies were motivated by the measurements of Xie and Zare in which the populations of the individual parity components of each ion rotational level were obtained using laser-induced fluorescence.<sup>10,11</sup> Such measurements of ion populations for individual parity components of a  $\Lambda$  doublet provide a very stringent test of the underlying angular momentum make-up of molecular photoelectron wave functions.<sup>9,10</sup> These spectra show a strongly (-) parity-favored ion rotational distribution for photoionization of the (+) parity component of the  $J = 4$  level of the 5p $\pi$  Rydberg orbital of the  $F^1\Delta_2$  state which has about 97% p ( $\ell = 1$ ) character. These (-) parity-favored ion distributions can be readily understood on the basis of parity selection rules<sup>12,13</sup> and the dominance of the photoelectron matrix element by its  $\ell = 0$  and 2 angular momentum components for photoionization

of this  $5p\pi$  Rydberg orbital with its 97% p character. Fig. 3 compares our calculated

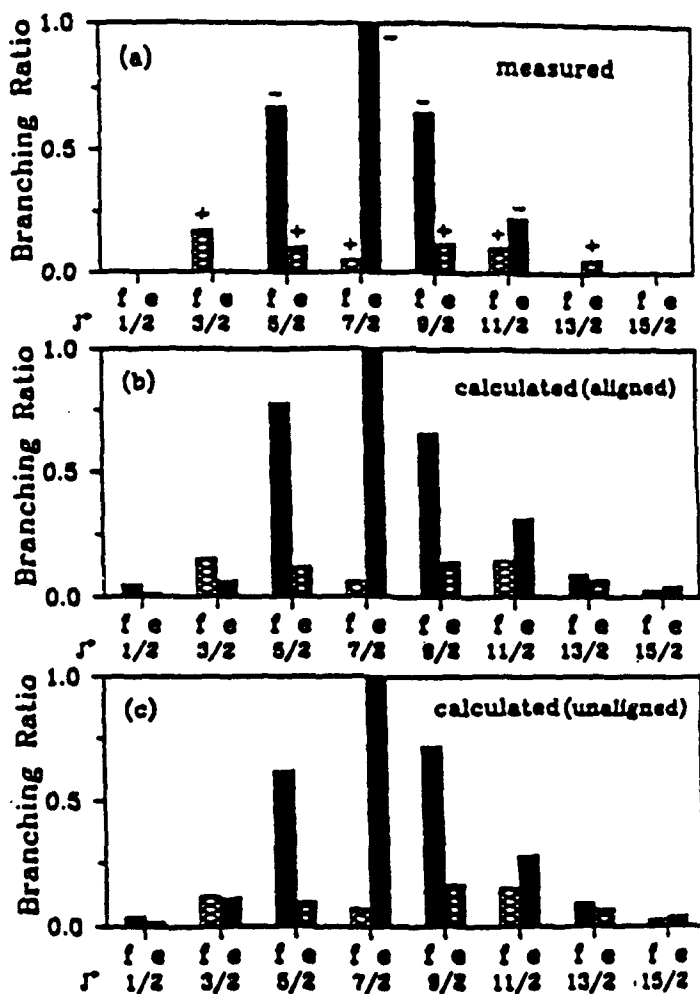


Fig. 3. Rotational distributions of  $\text{HBr}^+$  for  $(2 + 1)$  REMPI via the  $S(2)$  branch of the  $F\ 1\Delta_2$  state: (a) measured distributions of ref. 16; (b) and (c) calculated distributions of ref. 9 for the aligned and unaligned resonant states, respectively.

ion rotational distributions with the measured spectra of Xie and Zare.<sup>6</sup> The photo-electron energy is about 2.33 eV. Calculated spectra are shown for photoionization of both the optically aligned  $J = 4$  level (fig. 3(b)) and an unaligned  $J = 4$  level

(fig. 3(c)). The agreement between the calculated and measured ion distributions is very encouraging.

Note that, on the basis of parity selection rules,<sup>12,13</sup> the 20% population seen in the (+) parity component (cross-hatched bars) of the doublet *must be due to odd partial wave components of the photoelectron matrix element which arise from angular momentum coupling in the molecular photoelectron.* Examination of the photoelectron matrix elements reveals that the  $i$  wave of the  $5p\pi \rightarrow k\delta$  ionization channel makes the dominant contribution to the population of these (+) parity levels of the ion.<sup>9</sup> Such behavior is entirely nonatomic-like. Comparison of the ion distributions for the unaligned  $J = 4$  level with those for an optically aligned  $J = 4$  level and with the measured spectra serves to illustrate that, although not large, the effect of alignment can be important.

#### (b) *Threshold Photoionization of Linear Molecules*

We now highlight the progress we have made in our studies of ion rotational distributions for single-photon ionization of diatomic molecules and fragments by coherent VUV and XUV radiation. In contrast to the spectra discussed above where the photoelectron energies were of the order of 1 to 2 eV, we now look at ion rotational distributions for threshold photoionization where the photoelectron energy is essentially zero. The measured spectra with which our calculated ion rotational distributions will be compared in the two examples have been obtained using a technique based on the detection of zero-kinetic-energy (ZEKE) photoelectrons resulting from pulsed-field ionization (PFI) of very high Rydberg states lying below a rotational threshold.<sup>2</sup> This ZEKE-PFI technique makes it possible to obtain ion rovibronic state distributions with sub-wavenumber resolution. Although

these ZEKE techniques are limited to measurements of threshold photoionization cross sections, *this dramatic improvement in resolution over that of conventional photoelectron certainly opens up new possibilities for studying photoionization dynamics, ion spectroscopy, and state-selected ion-molecule reactions.* In fact, several novel applications built on the ultra-high resolution of this technique have already emerged.<sup>14</sup> Measurements of ion rotational distributions for very low rotational levels and at threshold photoelectron energies, which this technique makes possible for a wide range of molecules, can certainly be expected to raise important theoretical challenges and to provide significant insight into the coupling of electronic and nuclear motion inherent in the photoionization process.

Fig. 4 shows the (a) measured and (b) our calculated ZEKE photoelectron spectra for single-photon ionization of rotationally cold NO  $X^2\Pi_{1/2}, (v'' = 0)$  molecules leading to NO<sup>+</sup> ( $X^1\Sigma^+, v^+ = 1$ ) by coherent VUV radiation.<sup>15</sup> The calculated ion rotational distributions assume a temperature of 5 K. These spectra were calculated for a photoelectron energy of 50 meV and convoluted with a Gaussian detection function with an FWHM of  $2\text{ cm}^{-1}$ . In this figure each branch is associated with a letter designation which refers only to the change in angular momentum apart from spin, i.e.,  $\Delta N = N^+ - N''$ . The label 1' denotes the  $N'' = 1, J'' = 1/2$  level. The agreement between these measured and calculated spectra is excellent.

To provide further insight into the underlying dynamics of these threshold photoelectron spectra, fig. 5 (a) and (b) show measured and calculated ion rotational branching ratios for photoionization of the  $N'' = 1, J'' = 3/2$  rotational level of the  $X^2\Pi_{1/2}$  ground state of NO. The data of fig. 5 (a) is extracted from

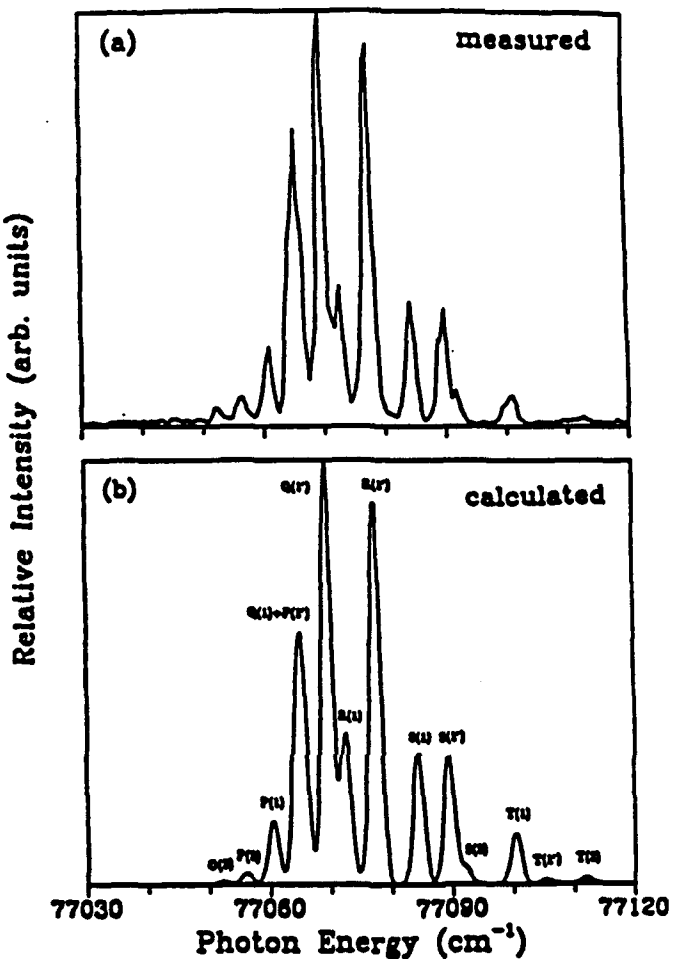


Fig. 4. (a) measured and (b) calculated ZEKE photoelectron spectra for single-photon ionization of rotationally cold NO ( $X^2\Pi_{1/2}$ ) by coherent VUV radiation. The calculated spectrum is for 5 K.

the measured photoelectron spectrum of fig. 4 (a) for rotationally cold NO where, in addition to the  $N'' = 1$  level, a few other rotational levels are also populated. These rotational branching ratios for ionization of this valence  $2\pi$  orbital differ somewhat from those generally seen in ZEKE spectra of Rydberg states. This behavior reflects the broad range of angular momentum components ( $\ell = 0, 1, 2$ , and 3) which

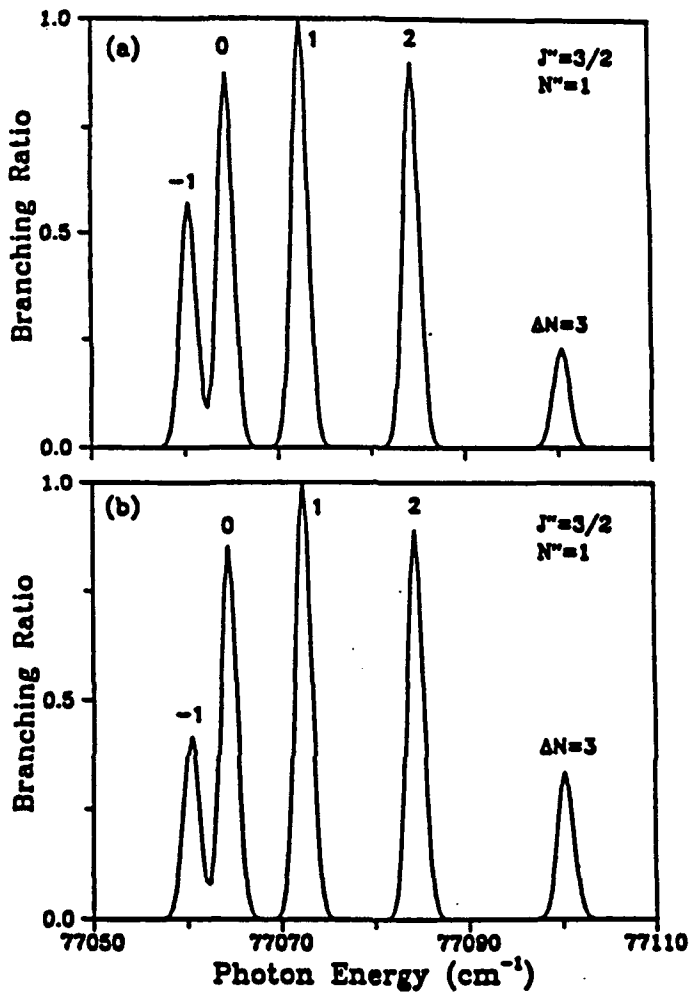


Fig. 5 (a) measured and (b) calculated ZEKE photoelectron spectra for single-photon ionization of the  $N'' = 1, J'' = 3/2$  level of the  $X^2\Pi_{1/2}$  state of NO by coherent UVU radiation.

make significant contributions to the photoelectron matrix element for this valence orbital. Unusually strong s and d waves are predicted in addition to the p and fpartial waves expected for photoionization of the  $2\pi$  orbital with its 85% d ( $\ell = 2$ ) character. These s and d components of the photoionization matrix element are due to angular momentum coupling in the molecular photoelectron wavefunction.

Fig. 6 shows the ZEKE photoelectron spectra for single-photon ionization of rotationally cold CO ( $X^1\Sigma^+$ ) molecules by coherent XUV radiation.<sup>16</sup> These jet-cooled PFI spectra are for the  $v^+ = 0$  level of CO<sup>+</sup> ( $X^2\Sigma^+$ ). The calculated spectra assume a temperature of 8 K and a photoelectron energy of 50 meV and are convoluted with a Gaussian detection function with an FWHM of

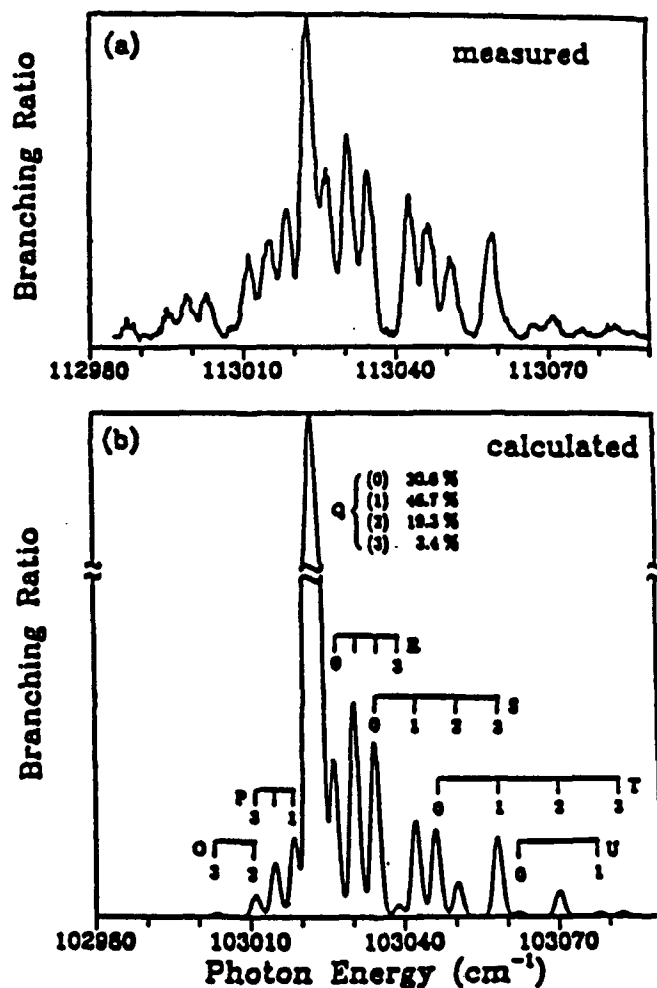


Fig. 6. (a) measured and (b) calculated ZEKE photoelectron spectra for single-photon ionization of rotationally cold CO ( $X^1\Sigma^+$ ) by coherent XUV radiation. The calculated spectrum is for 8 K.

$2 \text{ cm}^{-1}$ . The letter designation on each branch refers only to the change of angular momentum apart from spin. The agreement between these calculated and measured rotational branching ratios is excellent for all branches except the Q ( $\Delta N = 0$ ) branch. This behavior is indicated by the broken scale in fig. 6(b). The strength of the Q branches in these spectra is consistent with the parity selection rule,  $\Delta N + \ell = \text{odd}$ ,<sup>12</sup> and the atomiclike behavior for photoionization of the  $5\sigma$  orbital (45% s and 25% d character). The origin of this disagreement between these calculated and measured spectra is not yet clear.

(c) *Threshold Photoionization of Nonlinear Molecules*

Fig. 7 (a) shows the rotationally resolved ZEKE pulsed-field ionization spectrum of  $\text{H}_2\text{O}$  recently reported by Tonkyn et al. for single-photon ionization of the  $1\text{b}_1$  orbital by coherent VUV radiation<sup>17</sup>. This spectrum can be assigned to two types of rotational transitions, corresponding to specific changes in the asymmetric top angular momentum projection quantum numbers  $K_a$  and  $K_c$ . Most of the strong spectral lines could be classified as type c rotational transitions ( $\Delta K_a = \text{odd}$ ,  $\Delta K_c = \text{even}$ ), but type a transitions ( $\Delta K_a = \text{even}$ ,  $\Delta K_c = \text{odd}$ ) are also clearly evident. Fig. 7(b) shows our calculated ion rotational distributions for photoionization of the  $1\text{b}_1$  orbital of the  $\tilde{X}^1\text{A}_1$  ground state of jet-cooled  $\text{H}_2\text{O}$  leading to the  $\tilde{X}^2\text{B}_1$  (000) state of the ion.<sup>18</sup> A rotational temperature of 15 K is assumed in these calculations. Furthermore, we assume that there is no spin exchange taking place during the jet-cooled expansion of room-temperature water. The calculated spectrum is convoluted with a Gaussian detection function with an FWHM of  $1.5 \text{ cm}^{-1}$ . The agreement between the calculated and measured spectra is clearly encouraging except for the calculated  $0_{00} \rightarrow 2_{12}$  transition which is somewhat stronger than that

of the measured value.

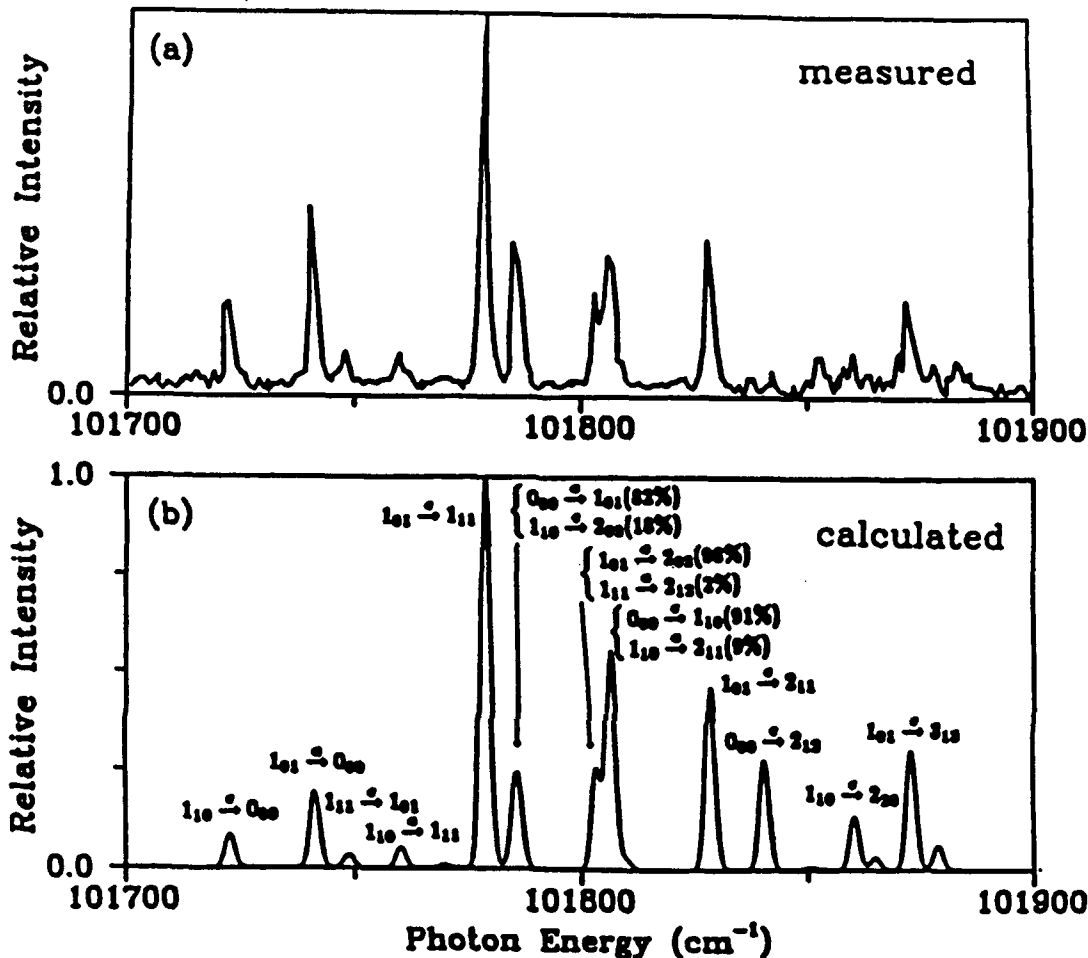


Fig. 7. (a) measured and (b) calculated ion rotational distributions for photoionization of the  $1b_1$  orbital of the  $\tilde{X}^1A_1$  ground state of jet-cooled  $H_2O$ . The *a* and *c* labels indicate type *a* and type *c* transitions, respectively.

The underlying dynamics of these photoelectron spectra is quite rich. We have shown that parity selection rules require that<sup>18,19</sup>

$$\Delta K_a + \ell = \text{odd}, \quad (2)$$

and

$$4\mu + \lambda = \Delta K_b, \quad (3)$$

where  $\mu$  is the photon polarization index in the molecular frame and  $\lambda$  is the projection of  $\ell$ , the angular momentum of the photoelectron, in the molecular frame.<sup>19</sup> Eqs. (2) and (3) assume that the molecular  $z$  axis coincides with the  $C_2$  symmetry axis and the  $x$  axis lies in the plane of the molecule. The molecular  $x$ ,  $y$ , and  $z$  axes hence coincide with the  $a$ ,  $c$ , and  $b$  axes, respectively. Since  $\mu + \lambda$  is always odd for photoionization of the  $1b_1$  orbital of  $H_2O$ , it can be shown that<sup>19</sup>

$$\Delta K_a + \Delta K_c = \text{odd}. \quad (4)$$

Both type  $a$  and type  $c$  transitions are allowed and type  $b$  [ $\Delta K_a = \text{even (odd)}$  and  $\Delta K_a = \text{even (odd)}$ ] transitions are forbidden. Furthermore, eq. 2 shows that *type a transitions* ( $1_{01} \rightarrow 0_{00}$ ,  $0_{00} \rightarrow 1_{01}$ ,  $1_{01} \rightarrow 2_{02}$ , and  $1_{11} \rightarrow 2_{12}$ ) *arise from odd (almost pure p) wave contributions to the photoelectron matrix element*. These  $p$  waves of the  $ka_1$  and  $kb_1$  continua are entirely molecular in origin since the almost  $p$  (99.7%) character of the  $1b_1$  orbital of water leads only to  $s$  and  $d$  photoelectron continua in an atomiclike picture. The strong type  $c$  transitions in the spectra of fig. 7 arise from  $s$  and  $d$  (even) components of the photoelectron matrix element.

Figure 8 shows the (a) measured<sup>20</sup> and (b) calculated<sup>21</sup> rotationally resolved ZEKE-PFI spectra of  $CH_3(\tilde{X}^2A''_2)$  for single-photon ionization of the  $1a''_2$  orbital by coherent VUV radiation leading to the  $\tilde{X}^1A'_1$  ground state of the ion. The calculated spectrum assumes a rotational temperature of 250 K and a photoelectron kinetic energy of 50 meV and is convoluted with a Gaussian detection function with an FWHM of  $2.5 \text{ cm}^{-1}$ . The  $CH_3$  and  $CH_3^+$  are oblate symmetric tops, belonging to the  $D_{3h}$  point group. For the  $D_{3h}$  group, the *total* wave function of  $CH_3$  should

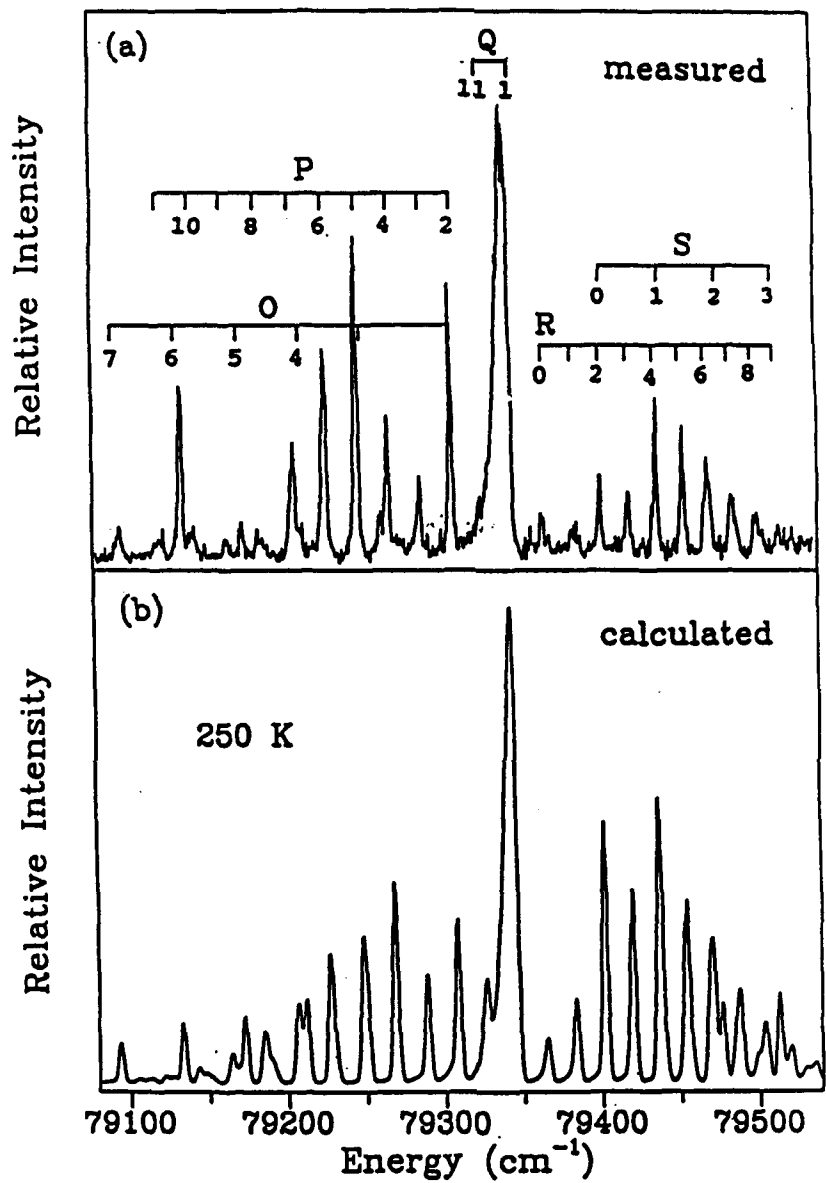


Fig. 8 (a) measured and (b) calculated ion rotational distributions for single-photon ionization of the  $1a''$  orbital of the  $\tilde{X}' 2 A''$  ground state of jet-cooled  $\text{CH}_3$  leading to the  $\tilde{X}' 1 A'$  ground state of the ion. The calculated spectrum is for 250 K and has an FWHM of  $2.5 \text{ cm}^{-1}$ .

have either  $A'_1$  or  $A''_2$  symmetry in order to satisfy the Pauli principle. The wave functions for ortho and para species have  $A'_1$  ( $I = 3/2$ ) and  $E'$  ( $I = 1/2$ ) symmetries,

respectively. Since  $\Gamma_{spin} \otimes \Gamma_{rot} \supset \Gamma_{total}$ , the rotational wave function must have  $A'_2$ ,  $A''_2$ ,  $E'$ , or  $E''$  symmetry. Therefore, the rotational levels belonging to  $A'_1$  and  $A''_1$  symmetries are not initially populated, i.e., levels with  $J = even$ ,  $K = 0$  and the  $A_1$  ( $K = 3n$ ) level of the  $A_1 - A_2$  pair are forbidden. Due to the spin statistical weight of 4:2 between ortho and para species, the  $K = 3n + 1$  levels ( $A'_2$  or  $A''_2$ ) have a statistical weight twice that of the  $K = 3n + 1$  levels ( $E'$  or  $E''$ ).

Agreement between the calculated and measured spectra is very encouraging in spite of some discrepancies due to rotational autoionization at negative  $\Delta N$  transitions. Our calculations reveal that  $\Delta K = 0$  are the dominant transitions (up to 95%) and the  $\Delta K = \pm 2$  (not labeled) transitions are much weaker. Even though the  $\Delta K = odd$  transitions are also dipole-allowed, their intensities are very weak and they do not appear in the spectrum. Note that  $\Delta K = odd$  transitions are associated with  $\mu + \lambda = odd$  partial waves of the photoelectron, which, in turn, must originate from the  $f$  ( $\ell_0 = 3$ ) component of the  $1a''_2$  orbital of the ground state. Since the  $1a''_2$  orbital is essentially an out-of-plane  $2p$  orbital localized on the central carbon atom, its  $f$  wave is negligible. This leads to a  $\Delta K = even$  selection rule.

Figure 9 shows the (a) measured and (b) calculated rotationally resolved ZEKE-PFI spectra of  $H_2CO$  for single-photon ionization of the nonbonding  $2b_2$  orbital by coherent VUV radiation.<sup>21</sup> The calculated spectrum assumes a rotational temperature of 7 K and a photoelectron kinetic energy of 50 meV and is convoluted with a Gaussian detection function with an FWHM of  $1.8 \text{ cm}^{-1}$ . Furthermore, we assume that no spin exchange takes place during the jet-cooled expansion of room-temperature formaldehyde, i.e., a population ratio of 2:1 is kept for the ortho (B

symmetry) to para (A symmetry) species. The agreement between calculated and measured spectra is very encouraging.

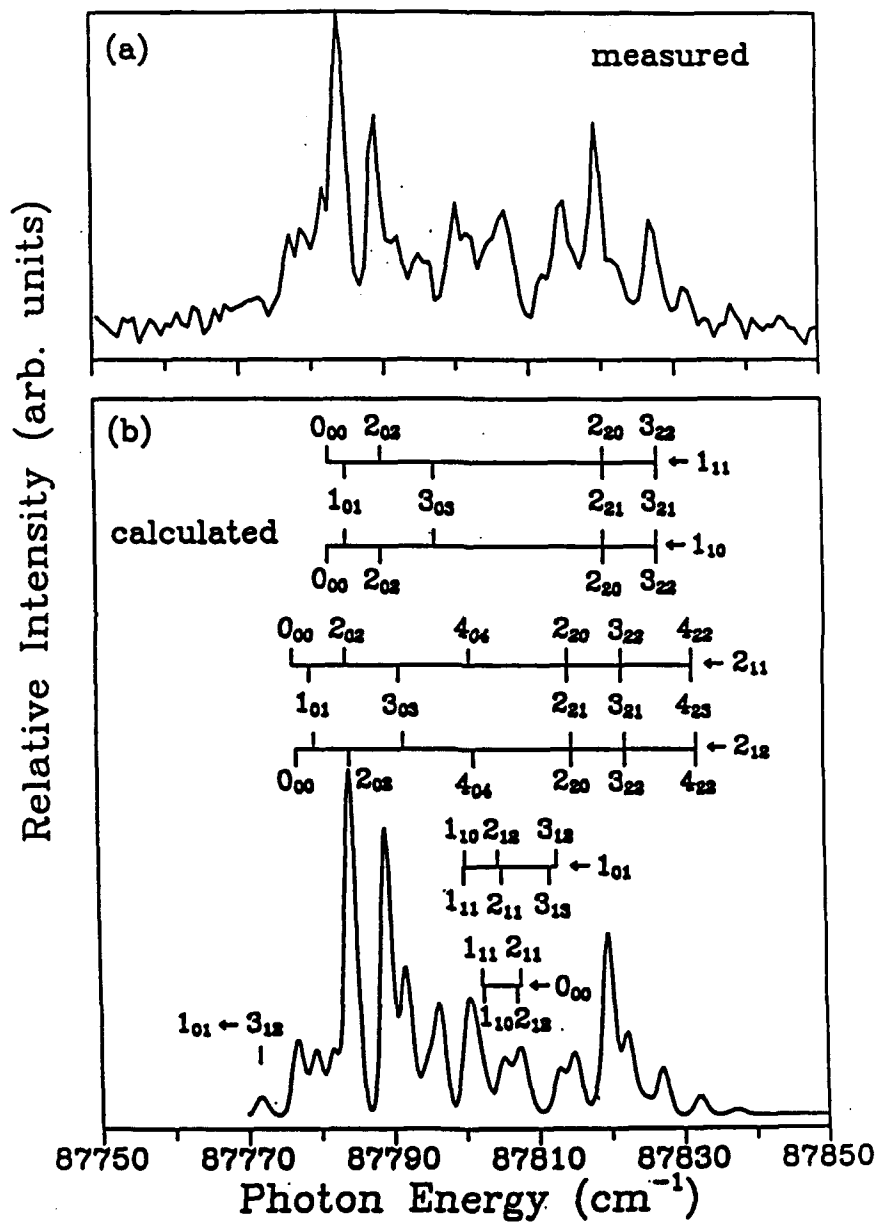


Fig. 9 (a) measured and (b) calculated ion rotational distributions for single-photon ionization of the  $2b_2$  orbital of the  $\tilde{X}^1A_1$  ground state of jet-cooled H<sub>2</sub>CO. The calculated spectrum is for 7 K and has an FWHM of 1.8  $\text{cm}^{-1}$ .

In our calculations we assume that the molecular  $z$  axis coincides with the  $C_2$  symmetry axis and the  $x$  axis lies in the plane of the formaldehyde molecule (ion). The molecular  $x$ ,  $y$ , and  $z$  axes hence coincide with the  $b$ ,  $c$ , and  $a$  axes, respectively. From the parity selection rules we obtain

$$\Delta K_b + \ell = \text{odd}, \quad (5)$$

and

$$\mu + \lambda = \Delta K_a. \quad (6)$$

From photoionization of the  $2b_2$  orbital of  $H_2CO$ ,  $\mu + \lambda$  is always odd and, hence, we have

$$\Delta K_b + \Delta K_c = \text{odd}. \quad (7)$$

Clearly, both type  $c$  ( $\Delta K_a = \text{odd}$  and  $\Delta K_c = \text{even}$ ) and type  $b$  ( $\Delta K_a = \text{odd}$  and  $\Delta K_c = \text{odd}$ ) transitions are allowed and type  $a$  ( $\Delta K_a = \text{even}$  and  $\Delta K_c = \text{odd}$ ) and other type  $b$  ( $\Delta K_a = \text{even}$  and  $\Delta K_c = \text{even}$ ) transitions are forbidden. Furthermore, Eqns. (5-7) show that the allowed type  $b$  transitions arise from odd partial wave contributions to the photoelectron matrix elements whereas the type  $c$  transitions arise from even angular momentum components of the photoelectron.

In Fig. 9 (b), we label several of the more important transitions out of rotational levels of the ground state of the neutral species leading to different rotational levels of the ion. The quantum numbers used as labels are  $N_{K_a K_c}$ . Note that in this figure we use the same set of quantum numbers to designate type  $c$  transitions out of the  $1_{11}$  level and type  $b$  transitions out of the  $1_{10}$  level, since the energies of these transitions are essentially equal. A similar labeling is also adopted for transitions out of the  $2_{11}$  and  $2_{12}$  rotational levels. Since the moments of inertia  $I_b$  and  $I_c$  are almost the same for  $H_2CO$  ( $H_2CO^+$ ), the rotationally resolved ZEKE-PFI spectra

are very congested. Unlike the spectra for H<sub>2</sub>O, type *b* transitions, which arise from odd waves, cannot be distinguished from type *c* transitions, which arise from even waves.

#### *References*

1. See, for example, R.G. Tonkyn and M.G. White, Rev. Sci. Instrum. **60**, 1245 (1989).
2. K. Müller-Dethlefs and E.W. Schlag, Ann. Rev. Phys. Chem. **42**, 109 (1991).
3. C.-W. Hsu, D.P. Baldwin, C.-L. Liao, and C. Y. Ng, J. Chem. Phys. **100**, 8047 (1994).
4. R. R. Lucchese, K. Takatsuka, and V. McKoy, Phys. Rept. **131**, 147 (1982).
5. E. de Beer, M. Born, C. A. de Lange, and N. P. C. Westwood, Chem. Phys. Lett. **186**, 40 (1991).
6. K. Wang, J. A. Stephens, V. McKoy, E. de Beer, C. A. de Lange, and N. P. C. Westwood, J. Chem. Phys. **97**, 211 (1991).
7. E. de Beer, C. A. de Lange, J. A. Stephens, K. Wang, and V. McKoy, J. Chem. Phys. **95**, 714 (1991).
8. H. Rudolph and V. McKoy, J. Chem. Phys. **91**, 7995 (1989).
9. K. Wang and V. McKoy, J. Chem. Phys. **95**, 7872 (1991).
10. J. Xie and R. N. Zare, Chem. Phys. Lett. **159**, 399 (1989).
11. J. Xie and R. N. Zare (private communication).
12. K. Wang and V. McKoy, J. Chem. Phys. **95**, 4977 (1991).
13. J. Xie and R. N. Zare, J. Chem. Phys. **93**, 3033 (1990).
14. See, for example, E. R. Grant and M. G. White, Nature **354**, 249 (1991).
15. R. Wiedmann, M. G. White, K. Wang, and V. McKoy, J. Chem. Phys. **97**, 9874 (1993).

16. K. Wong, D. Rodgers, J. W. Hepburn, K. Wang, and V. McKoy, *J. Chem. Phys.* **97**, 3159 (1993).
17. R. G. Tonkyn, R. T. Wiedmann, E. R. Grant, and M. G. White, *J. Chem. Phys.* **95**, 7033 (1991).
18. M.-T. Lee, K. Wang, V. McKoy, R. G. Tonkyn, R. T. Wiedmann, E. R. Grant, and M. G. White, *J. Chem. Phys.* **96**, 7848 (1992).
19. M.-T. Lee, K. Wang, and V. McKoy, *J. Chem. Phys.* **97**, 3108 (1992).
20. J. A. Blush, P. Chen, R. T. Wiedmann, and M. G. White, *J. Chem. Phys.* **98**, 3557 (1993).
21. R. T. Wiedmann, M. G. White, K. Wang, and V. McKoy, *J. Chem. Phys.* **100**, 4738 (1994).

**III    *The research highlighted above has resulted in the following publications:***

1. *Rotationally Resolved Photoionization of Polyatomic Hydrides: CH<sub>3</sub>, H<sub>2</sub>O, H<sub>2</sub>S, H<sub>2</sub>CO*  
R.T. Wiedmann, M. White, K. Wang, and V. McKoy  
*J. Chem. Phys.* **100**, 4738 (1994)
2. *Rotationally Resolved Threshold Photoelectron Spectroscopy of H<sub>2</sub>O and H<sub>2</sub>S*  
K. Wang, M.-T. Lee, V. McKoy, R.T. Wiedmann, and M. White  
*Chem. Phys. Lett.* **219**, 397 (1994)
3. *Studies of Photoionization Dynamics of CH, NH, and OH Radicals at Near-Threshold Photoelectron Kinetic Energies*  
K. Wang, J.A. Stephens, and V. McKoy  
*J. Phys. Chem.* **98**, 460 (1994)
4. *Pulsed-Field Ionization Threshold Photoelectron Spectroscopy with Coherent XUV Radiation: A Comparison of CO and N<sub>2</sub>*  
W. Kong, D. Rodgers, J.W. Hepburn, K. Wang, and V. McKoy  
*J. Chem. Phys.* **99**, 3159 (1993)

5. *Energy Dependence of Photoion Rotational Distributions of N<sub>2</sub> and C<sub>2</sub>*  
Heung Cheun Choi, R.M. Rao, A.G. Mihill, Sandeep Kakar, E.D. Poliakoff,  
K. Wang, and V. McKoy  
Phys. Rev. Lett. **72**, 44 (1994)

6. *Spin-Orbit Autoionization and Intensities in the Double-Resonant Delayed Pulsed-Field Threshold Photoionization of HCl*  
Y.-F. Zhu, E.R. Grant, K. Wang, and V. McKoy  
J. Chem. Phys. **100**, 8633 (1994)

7. *Rotationally Resolved Photoelectron Spectra in (2+1) Resonance Enhanced Multiphoton Ionization of NO via the C 2Π Rydberg State*  
K. Wang, V. McKoy, and H. Rudolph  
Chem. Phys. Lett. **216**, 490 (1993)

8. *Rotationally Resolved Photoelectron Spectra at Near-Threshold Kinetic Energies*  
K. Wang and V. McKoy  
Highly Resolved Laser Photoionization and Photoelectron Studies  
edited by I. Powis (John Wiley, 1994)

9. *Ion Rotational Distributions for Nonlinear Molecules at Near-Threshold Photoelectron Energy*  
K. Wang and V. McKoy  
Proceedings of the SPIE Laser Symposium on Laser Techniques for  
State-Selected and State-to-State Chemistry  
(Los Angeles, 1993), p. 257

10. *Single-Photon Threshold Photoionization of NO*  
R. T. Wiedmann, M. White, K. Wang, and V. McKoy  
J. Chem. Phys. **98**, 7673 (1993)

11. *Rotational State-Selective Photoionization Dynamics of Molecules at Near-Threshold Photoelectron Energies*  
K. Wang, J. Stephens, and V. McKoy  
J. Phys. Chem. **97**, 9874 (1993)

**12. Rotational Analysis of the HeI Photoelectron Spectrum of HF**  
K. Wang, V. McKoy, M.-W. Ruf, A.J. Yencha, and H. Hotop  
*J. Electron Spectroscopy and Related Phenomena* **63**, 11 (1993)

**13. Studies of Molecular Rydberg States by Schwinger Variational-Quantum Defect Methods: Application to Molecular Hydrogen**  
J.A. Stephens and V. McKoy  
*J. Chem. Phys.* **97**, 8060 (1992)

**14. Ion-Rotational Distributions at Near-Threshold Photoelectron Energies**  
K. Wang, J. Stephens, and V. McKoy  
Vacuum Ultraviolet Radiation Physics, Proceedings of the  
10th VUV Conference, (Paris, July 27-31, 1992), edited by  
F.J. Wuilleumier, Y. Petroff and I. Nenner  
(World Scientific Publishing : Singapore), 1993, p. 247

**15. Rotationally Resolved Photoelectron Spectra in Resonance Enhanced Multiphoton Ionization of SiF**  
K. Wang and V. McKoy  
*J. Chem. Phys.* **97**, 5489 (1992)

**16. Rotationally Resolved Photoelectron Spectra in Resonance Enhanced Multiphoton Ionization of H<sub>2</sub>O via the C<sup>1</sup>B<sub>1</sub> Rydberg State**  
M.-T. Lee, K. Wang, V. McKoy, and L. E. Machado  
*J. Chem. Phys.* **97**, 3905 (1992)

**17. Rotationally Resolved Near-Threshold Photoionization of the 1b<sub>1</sub> Valence Orbital of H<sub>2</sub>O and D<sub>2</sub>O**  
M.-T. Lee, K. Wang, and V. McKoy  
*J. Chem. Phys.* **97**, 3108 (1992)

**18. Rotationally Resolved Photoelectron Spectra in Resonance Enhanced Multiphoton Ionization of Rydberg States of NH**  
K. Wang, J.A. Stephens, V. McKoy, E. de Beer,  
C.A. de Lange, and N.P.C. Westwood  
*J. Chem. Phys.* **97**, 211 (1992)

19. *Rotationally Resolved Threshold Photoelectron Spectra of OH and OD*  
R.T. Wiedmann, R.G. Tonkyn, M.G. White, K. Wang, and V. McKoy  
*J. Chem. Phys.* **97**, 768 (1992)

20. *Ion Rotational Distributions for Near-Threshold Photoionization of H<sub>2</sub>O*  
M.-T. Lee, K. Wang, V. McKoy, R.G. Tonkyn, R.T. Wiedmann,  
E.R. Grant, and M.G. White  
*J. Chem. Phys.* **96**, 7848 (1992)

21. *Rotationally Resolved Photoelectron Spectra in Resonance Enhanced Multiphoton Ionization of HCl via the f <sup>1</sup>Δ<sub>2</sub> Rydberg State*  
K. Wang and V. McKoy  
*J. Chem. Phys.* **95**, 8718 (1991)

22. *Rotationally Resolved Photoionization of Molecular Oxygen*  
M. Braunstein, V. McKoy, and S.N. Dixit  
*J. Chem. Phys.* **96**, 5726 (1992)

23. *Rotational Branching Ratios and Photoelectron Angular Distributions in Resonance Enhanced Multiphoton Ionization of HBr via the f <sup>1</sup>Δ<sub>2</sub> Rydberg State*  
K. Wang and V. McKoy  
*J. Chem. Phys.* **95**, 7872 (1991)

24. *Effects of Cooper Minima in Resonance Enhanced Multiphoton Ionization Photoelectron Spectroscopy of NO via the D <sup>2</sup>Σ<sup>+</sup> and C <sup>2</sup>Π Rydberg States*  
K. Wang, J.A. Stephens, and V. McKoy  
*J. Chem. Phys.* **95**, 6456 (1991)

25. *Rotational Branching Ratios and Photoelectron Angular Distributions in Resonance Enhanced Multiphoton Ionization of Diatomic Molecules*  
K. Wang and V. McKoy  
*J. Chem. Phys.* **95**, 4977 (1991)

26. *Rotationally Resolved Photoelectron Spectroscopy of the <sup>2</sup>Σ<sup>-</sup> Rydberg States of OH: The Role of Cooper Minima*

E. de Beer, C.A. de Lange, J.A. Stephens, K. Wang,  
and V. McKoy  
J. Chem. Phys. 95, 714 (1991)

27. *Cooper Minima and Circular Dichroism in Photoelectron Angular Distributions*

H. Rudolph, R.L. Dubs, and V. McKoy  
J. Chem. Phys. 93, 7513 (1990)

28. *Non-Franck-Condon Effects in Photoionization of the  $g\ 3\Pi$  Rydberg State of NH*

K. Wang, J. A. Stephens, and V. McKoy  
J. Chem. Phys. 93, 7874 (1990)

29. *Orbital Evolution and Promotion Effects in the Photoionization Dynamics of  $^2\Sigma^-$  Rydberg States of OH*

J. A. Stephens and V. McKoy  
J. Chem. Phys. 93, 7863 (1990)

30. *Shape Resonance Effects in the Rotationally Resolved Photoelectron Spectra of O<sub>2</sub>*

M. Braunstein, V. McKoy, S.N. Dixit, R.G. Tonkyn, and M.G. White  
J. Chem. Phys. 93, 5345 (1990)

31. *(2+1') Rotationally Resolved Resonance Enhanced Multiphoton Ionization via the E  $^2\Sigma^+$  (4s, 3d) and H  $^2\Sigma^+$  (3d, 4s) Rydberg States of NO*

H. Rudolph and V. McKoy  
J. Chem. Phys. 93, 7054 (1990)

**IV Seminars and invited lectures presented on the studies outlined above include:**

1. Invited speaker at the Gordon Research Conference on Multiphoton Processes, June 1990, Colby-Sawyer Junior College, New Hampshire
2. Invited speaker at the European Research Conference on Very High Resolution Spectroscopy with Photoelectrons-ZEKE Spectroscopy, October 1991, Kreuth, Germany.

**Note:** The European Research Conferences are Gordon-like Research Conferences sponsored by the European Science Foundation and the Commission of the European Communities.

3. Invited Speaker at the 10th International Conference on Vacuum Ultraviolet Radiation Physics, July 1992, Paris, France
4. Invited Speaker at the International Workshop on Photoionization, August 1992, Berlin, Germany.  
*Note:* This Workshop is a *by-invitation-only* meeting covering significant developments in the field.
5. Invited Speaker at the annual meeting of the Division of Atomic, Molecular, and Optical Physics of the American Physical Society, May 1993, Reno, Nevada
6. Invited Speaker at the SPIE Laser Symposium on Techniques for State-Selected and State-to-State Chemistry, January 1993, Los Angeles, California
7. Invited Speaker at the European Research Conference on Very High Resolution Spectroscopy with Photoelectrons: Excited State Spectroscopy and Dynamics, September 1993, Giens, France
8. Plenary Speaker at the Sanibel Symposium on Photoinduced Phenomena, March 1992, St. Augustine, Florida
9. Colloquium Speaker at the University of Nebraska, Lincoln, Nebraska, September 1991
10. Colloquium Speaker at Louisiana State University, Baton Rouge, Louisiana, February 1992
11. Colloquium Speaker at the University of Waterloo, Waterloo, Ontario, June 1993
12. Distinguished Lecture Series: Frontiers in Chemical Research, Texas A&M University, December 1993

- 13. Colloquium Speaker at Tulane University, New Orleans, Louisiana, April 1994**
- 14. Invited Speaker at the European Workshop on Ion Spectroscopy, Tegernsee, Germany, September 1994**
- 15. Invited Speaker at the International Workshop on Photoionization, San Francisco, California, October 1994**

**IV The following graduate student was partially supported by this contract**

**Matthew Braunstein (1990-91)**

**The following research fellows were partially supported by this contract**

**J. A. Stephens**

**K. Wang**